

Interaction Between a Building Complex with an Integrated Thermal Energy System and a District Heating System

Daniel Rohde^{#1}, Trond Andresen^{*2}, Natasa Nord^{#3}

[#]*Department of Energy and Process Engineering
Norwegian University of Science and Technology
Kolbjørn Hejes vei 1A, 7491 Trondheim, Norway*

¹daniel.rohde@ntnu.no

³natasa.nord@ntnu.no

^{*}*SINTEF Energy Research
Sem Sælands vei 11, 7034 Trondheim, Norway*

²trond.andresen@sintef.no

Abstract

Integrated thermal energy systems provide heating and cooling for several commercial and residential buildings. These systems usually have both short-term and seasonal thermal energy storages. High cooling demands lead to a big amount of excess heat. This heat could be exported to a district heating system. Low temperature district heating can increase the integration of renewable and waste energy sources and may significantly contribute to the overall efficiency of future energy systems. In this study, the interaction of an integrated thermal energy system in Norway with district heating was investigated. The main parts of the energy system were heat pumps with 1 MW total cooling capacity, solar thermal collectors as well as water tanks and boreholes for thermal energy storage. It was assumed that heat from the solar collector tank could be exported to the district heating supply line, while the condenser heat from the heat pump was considered to be exported to the return line. Dynamic simulations were performed using a Modelica model of the energy system. An important result of the system simulations was the energy balance of the borehole thermal energy storage. Without heat export, the storage was charged more during summer than it was discharged during winter. This imbalance could lead to a ground temperature increase. To ensure feasible long-term operation of the energy system, the average annual ground temperature should remain constant. By exporting heat to the district heating system, borehole heat balance could be achieved and operating costs could be reduced.

Keywords - Integrated thermal energy system; District heating; Interaction; Dynamic simulation

1. Introduction

Integrated thermal energy systems provide heating and cooling for several commercial and residential buildings. In this study, the interaction of an integrated thermal energy system in Norway with a district heating (DH)

system was investigated. Due to high DH temperatures, the real system can only import heat. However, a technology shift towards low temperature DH systems is ongoing. This will lead to an increased integration of renewable and waste energy sources and may significantly contribute to the overall efficiency of future sustainable energy systems [1-3]. Therefore, a case study was defined with lower DH temperatures to investigate the possibility for export of excess heat from the building complex to the DH system.

2. Case Study

The basis for this case study was a thermal energy system that was integrated into a building complex of different building types with a total area of 38 000 m². The main parts of the energy system were heat pumps with 1 MW total cooling capacity, flat plate solar thermal collectors as well as water tanks and boreholes for thermal energy storage. The system is described in detail in [4] and a simplified version was modeled in Dymola/Modelica. The main system modifications and all investigated cases are explained in this chapter.

Hourly energy demand data from 2015 was used as input for the simulation model and the resulting monthly demands are shown in Figure 1. The demand for domestic hot water (DHW) varied significantly between 2014 and 2015 and so an average was used to give a representative demand profile for the building complex.

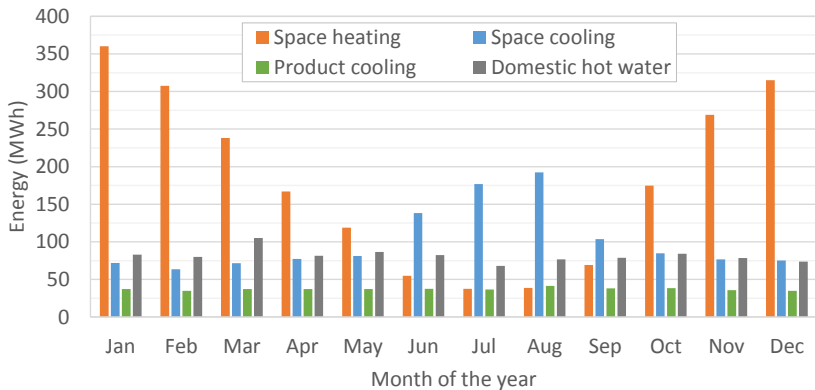


Figure 1: Monthly heating and cooling demands for the case study

To investigate the effects of changes in average annual temperatures, a warmer and a colder year were also simulated. For the warmer year, a temperature offset of +1°C, a radiation factor of 1.05, a space heating demand factor of 0.95 and a space cooling demand factor of 1.05 were used. Accordingly, a temperature offset of -1°C, a radiation factor of 0.95, a space heating demand factor of 1.05 and a space cooling demand factor of 0.95 were

implemented for the colder year. The average, warmer, and colder year simulations were respectively defined as Cases 1, 2, and 3, as shown in Table 1. The annual energy balance of the system's borehole thermal energy storage (BTES) was an important result for these cases.

Table 1: Case overview

Case	Year	Solar Collectors	Heat Export
1	Average	140	No export
2	Warmer	140	No export
3	Colder	140	No export
4	Average	140	To DH return line
5	Average	500	To DH supply and return line

The real system had five heat pumps connected in parallel and series. The condenser heat from all of them was led to the same secondary fluid loop. To simplify the control of the system, the heat pumps were modeled as one large heat pump. The system was connected to the local DH system to import heat for DHW heating and as backup for space heating. The outdoor temperature compensation curve is given in Figure 2.

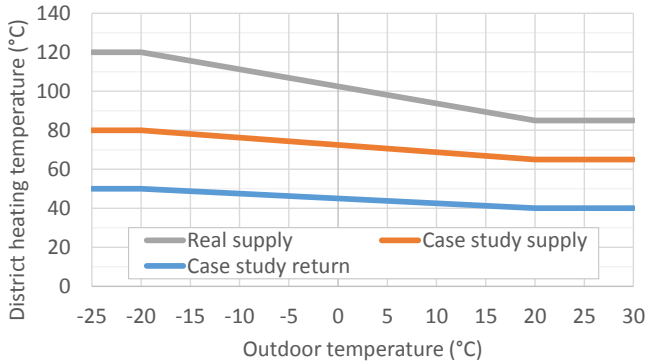


Figure 2: DH outdoor temperature compensation curves

The temperatures of the real DH system were too high to export heat economically even during summer. Therefore, a DH case was defined with lower supply and return temperature as shown in Figure 2. These temperatures represent a third generation system (“Scandinavian district heating technology” [2]) and were chosen because they satisfied the system’s temperature requirement for DHW heating ($>60^{\circ}\text{C}$), but also enabled export of excess heat from the building complex to the DH system.

To investigate export of excess heat, Cases 4 and 5 (see Table 1) were defined. For Case 4, heat export from the heat pump condenser tank to the DH

return line was enabled. For Case 5, heat export from the solar collector tank to the DH supply line was enabled. The amount of exported heat was controlled to yield a balanced BTES at the end of the year for both cases.

The real system had 140 solar collectors for space heating and DHW heating. However, this number was chosen based on the demand of only one single building and not the whole building complex. They were also only used within that building and thus showed little effect on the overall system performance. Therefore, the collector loop was connected to all buildings for Cases 4 and 5. Also, the number of solar collectors was increased to 500 and the volume of the collector tank was increased from 2 m³ to 10 m³ for Case 5.

3. Model Description

All simulation models were developed using the open modeling language Modelica with the *Thermal* library [5] as basis for component and system development. Dymola was used as simulation environment and the main component models and the control system are described here.

3.1. Component Models

The heat exchangers were modelled as an array of thermally connected pipes in counterflow configuration, where the local heat balance was solved in each element. A discretization of eight was found to give good agreement with logarithmic mean temperature calculations at reasonable simulation times. The heat transfer coefficient was chosen to be constant and equal in all array segments.

The BTES was modelled as an array of vertical segments. Each segment consisted of several thermal resistances and capacities. The resistances and capacities representing the ground heat exchanger were modelled according to [6]. The surrounding ground was modelled as an array of cylindrical shells with capacities and heat transfer coefficients corresponding to the geometry of each shell element according to [7].

The interaction between the boreholes and heat transfer to the ambient were neglected in the model. The horizontal ground discretization was found to be more important than the vertical discretization. Discretization values of sixteen (horizontal) and eight (vertical) were found to give good agreement with higher values at significantly reduced simulation times.

The heat pump was a key component and it was therefore desirable to include a model that realistically predicted performance and behavior under variable operating conditions. As an efficient means to introduce realistic off-design performance, the in-house circuit simulation and optimization tool *CSIM* [8] was used to generate a polynomial function to include in the Modelica model. *CSIM* has been developed by SINTEF and the Norwegian University of Science and Technology over the last decades.

The heat pump's coefficient of performance (COP) was defined as function of the scaled condenser heat load Q_s and the scaled temperature lift

ΔT_s . These parameters were considered key factors for heat pump performance and are defined in (1) and (2). The temperature lift ΔT was defined as the difference between average secondary fluid temperature in the condenser and average secondary fluid temperature in the evaporator. The nominal values used for scaling were parameters from the heat pumps design point.

$$Q_s = Q_{\text{actual}}/Q_{\text{nominal}} \quad (1)$$

$$\Delta T_s = \Delta T_{\text{actual}}/\Delta T_{\text{nominal}} \quad (2)$$

$$\text{COP} = \text{COP}_{\text{nominal}} \cdot (a + b \cdot Q_s + c \cdot \Delta T_s + d \cdot Q_s \cdot \Delta T_s) \quad (3)$$

More than 50 detailed simulations were performed with *CSIM* to map COP for conditions in the targeted operating range. A regression analysis was performed to find the coefficients for the polynomial function (3) and the resulting coefficients can be seen in Table 2.

Table 2: Parameters for polynomial heat pump model

Coefficient	a	b	c	d
Value	2.2451	-0.5868	-0.9228	0.2647

The resulting expression was implemented in the Modelica model and predicted the COP to within $\pm 5\%$ compared to the detailed simulation results from *CSIM*.

The solar collectors were modelled as fluid pipes which were heated by solar radiation. To account for heat transfer with the ambient, a constant value for thermal conductance from fluid to ambient was included. This value was chosen based on manufacturer specifications. The average error for the collector efficiency under different operating conditions was 2% with the parameters shown in Table 3.

Table 3: Solar collector model parameters (single collector)

Parameter	Value	Unit
Effective surface area	1.9	m ²
Optical efficiency	0.773	-
Fluid filling	1.2	kg
Thermal conductance (fluid to ambient)	8.6	W/K

The solar radiation was not measured on site, so data from the software *Meteonorm* was used as input for the simulations.

The thermal storage tanks were modeled to be perfectly mixed, i.e. without stratification. The thermal conductance from fluid to ambient was chosen to yield a capacity loss of 1% during a twelve hour period which is feasible according to [9].

3.2. Control System

A key part of the system modeling was the control system. Simple pump models were used to control the fluid flows between the components. The signals for activation of the pumps and the setpoints of their controllers were received from control blocks.

The system had two main modes of operation: Heating mode and cooling mode. The temperatures in the tanks after the heat pump's condenser and evaporator were used to define the mode of operation. In heating mode, the condenser tank was kept at a constant temperature (50°C) by the heat pump's PI controller and the evaporator tank and the BTES were used as heat sources. When the cooling load increased, the temperature in the evaporator tank also increased until the BTES was no longer needed as heat source. If the temperature in the tank reached a certain limit, the system switched to cooling mode, keeping the evaporator tank at a constant temperature (5°C). The condenser tank and the BTES were then used as heat sinks. Similarly, increasing heating loads led to a decreased temperature in the condenser tank and at a certain limit, the system switched to heating mode. The parameters for the heat pump's PI controller were chosen according to rules from [10] and blocks from the *StateGraph* library [11] were used to switch between modes.

The solar collector loop included two heat exchangers. The first one enabled heat transfer to the collector tank while the second one enabled heat transfer to the BTES. The control system was designed to transfer as much heat as possible to the collector tank at high temperature and only store low grade heat in the BTES. The fluid in the collector tank was then used for lifting the DHW temperature or heat export to the DH supply line, depending on the case. The DHW demand was prioritized to reduce the amount of imported heat. The control block settings had a significant influence on the total amount of accumulated solar heat and thus also on the energy balance of the system, especially for the case with increased number of collectors.

4. Results and Discussion

4.1. Energy Flows in the Integrated Thermal Energy System

For Case 1 (see Table 1), the BTES was charged with 799 MWh during summer and 602 MWh were discharged during winter. This imbalance of 197 MWh corresponds to an average ground temperature increase of almost 1°C. To ensure feasible long-term operation of the energy system, the average annual ground temperature should remain constant. For the simulated warmer year (Case 2), the imbalance was 350 MWh and 47 MWh for the colder year (Case 3). This clearly showed a potential for heat export.

Cases 1, 4 and 5 had the same weather and demand inputs and their total accumulated energies are shown in Figure 3. It can be seen that the heat pump is by far the most significant component, because it used the highest amount of energy.

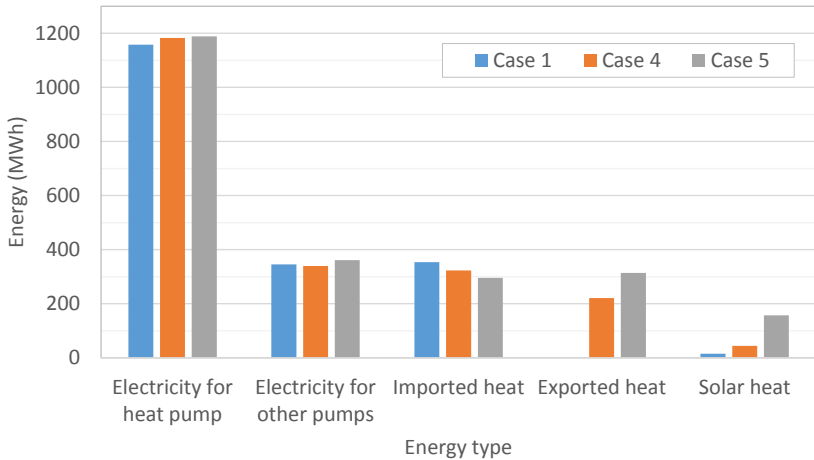


Figure 3: Total energy amounts for cases 1, 4, and 5

The electricity use of the system increased for the heat export Cases (4 and 5) compared to Case 1. At the same time, less heat needed to be imported due to better utilization of the solar collectors. As expected, more heat could be exported when the number of solar collectors was increased. Monthly values for the interaction with the DH system are shown in Figure 4.

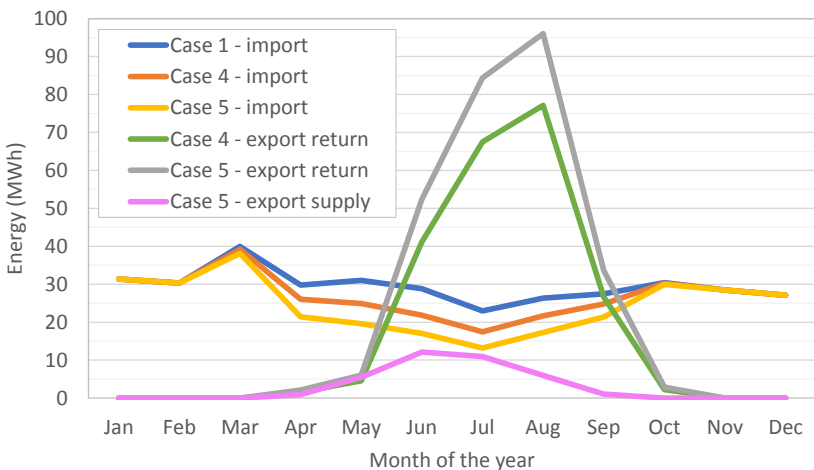


Figure 4: Monthly imported and exported heat for Cases 1, 4, and 5

It can be seen from Figure 4 that no heat was exported during winter because the system was in heating mode and did not have any excess heat

available. Heat import could not be avoided during summer even for Case 5. This was mainly due to the typical demand peak for DHW in the morning. This can be seen in Figure 5 which shows daily average profiles for a year.

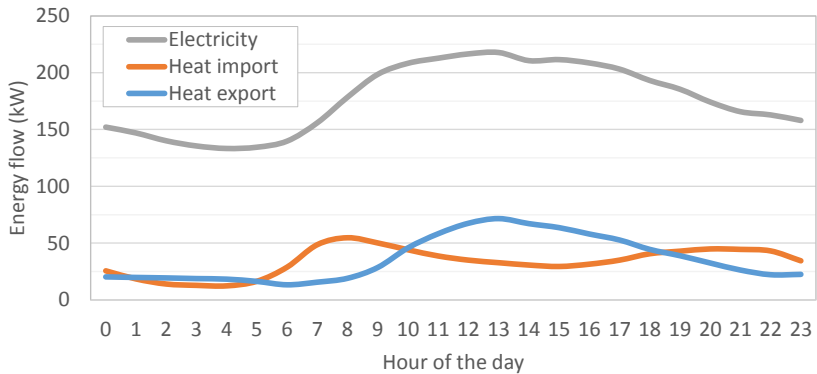


Figure 5: Daily average energy flows for different energy types over a year (Case 5)

It is not reasonable to reduce this import peak by storing high temperature solar heat during the night as this would lead to unnecessarily high losses. This can also be seen in Figure 6.

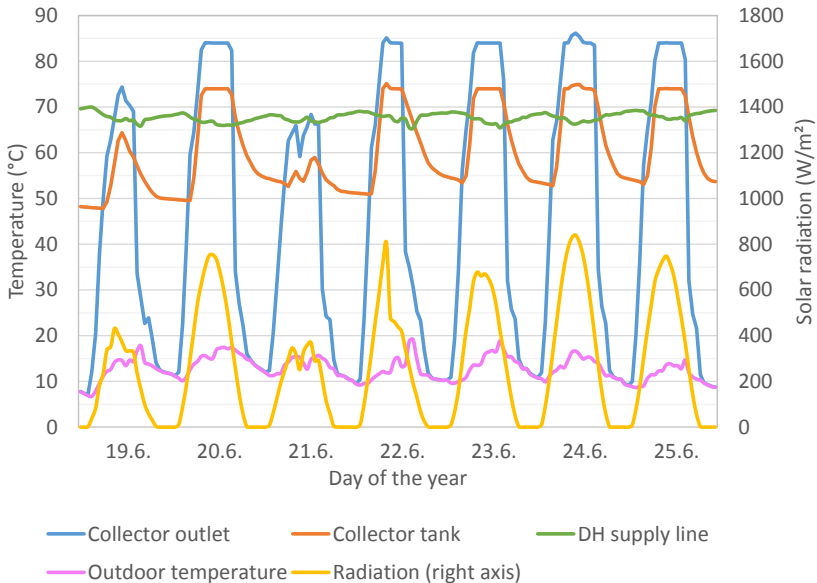


Figure 6: Solar collector loop details for one week (Case 5)

Figure 6 shows the temperatures of the collector tank loop for the period of one week. During the night, the collectors cool down to the outdoor temperature level and the temperature in the storage tank also decreases.

Heat export to the supply line was only possible when the temperature difference between collector tank and DH supply line exceeded the set threshold. Figure 6 shows that this was only the case during a few hours on clear summer days.

4.2. Cost Analysis

To compare the total operating costs of all the cases, price factors for the different energy types in Figure 3 were defined and are shown in Table 4.

Table 4: Price factors for different energy types

Energy Type	Electricity	DH import	DH export to supply	DH export to return
Price Factor	1.00	0.95	0.80	0.40

With these factors, the total operating costs compared to Case 1 were calculated and the results are shown in Table 5.

Table 5: Total operating costs compared to Case 1

Case	1	2	3	4	5
Operating costs	100 %	97.5 %	103 %	94.6 %	91.8 %

Energy prices for both electricity and DH vary significantly over time. However, this was not treated in the current study, due to the complexity of pricing mechanisms [12]. Therefore, the current results can only give an indication of the real costs and advantages of heat export. They showed that the influence of changed weather and demands (Cases 1 to 3) is rather small if the BTES is not balanced. However, depending on the heat losses from the storage (e.g. from ground water flow), this may not be feasible in the long run because the storage could overheat. Also, the operating costs for the heat export cases (4 and 5) were lower than for Case 1 so the only disadvantage are the higher installation costs. These are expected to be especially high for Case 5 which has the lowest operating costs. An economic analysis with more detailed pricing schemes is thus required to make recommendations for an improved system operation.

5. Conclusions

The interaction of a building complex with an integrated thermal energy system and a district heating system was analyzed. It was shown that the seasonal thermal energy storage could be balanced by exporting heat if the DH temperatures were lower than they are for the real system. Dynamic

simulations were performed and the results showed that the total operating costs decreased when heat was exported. A further decrease in operation cost could be achieved by increasing the number of solar collectors. Installation costs for heat export and increased collectors were not considered.

Acknowledgment

The authors gratefully acknowledge the support from the Research Council of Norway (INTERACT 228656 / E20) and the partners Aspelin Ramm Eiendom AS, Statkraft Varme AS, Rema 1000 Norge AS, COWI AS, Asplan Viak AS and SWECO.

References

- [1] D. Connolly, H. Lund, B.V. Mathiesen, S. Werner, B. Möller, U. Persson, T. Boermans, D. Trier, P.A. Østergaard, and S. Nielsen. *Heat Roadmap Europe: Combining district heating with heat savings to decarbonise the EU energy system*. Energy Policy, 2014. 65: p. 475-489.
- [2] H. Lund, S. Werner, R. Wiltshire, S. Svendsen, J.E. Thorsen, F. Hvelplund, and B.V. Mathiesen. *4th Generation District Heating (4GDH): Integrating smart thermal grids into future sustainable energy systems*. Energy, 2014. 68: p. 1-11.
- [3] D. Schmidt, A. Kallert, M. Blesl, S. Svendsen, N. Nord, and K. Sipilä. *Low temperature district heating for future energy systems*. The 14th International Symposium on District Heating and Cooling, Stockholm, Sweden. September 7-9, 2014.
- [4] D. Rohde, M. Bantle, T. Andresen, and N. Nord. *Documentation of an Integrated Thermal Energy System for a Building Complex*. 24th International Congress of Refrigeration, Yokohama, Japan. August 16-22, 2015.
- [5] Modelica Association. *Modelica Libraries*. Available from: <https://www.modelica.org/libraries>, accessed January 2016.
- [6] D. Bauer, W. Heidemann, H. Müller-Steinhagen, and H.J.G. Diersch. *Thermal resistance and capacity models for borehole heat exchangers*. International Journal of Energy Research, 2011. 35(4): p. 312-320.
- [7] P. Stephan. *Chapter B1: Fundamentals of Heat Transfer*, in *VDI Heat Atlas*. Springer Berlin Heidelberg. 2010.
- [8] T. Andresen. *Mathematical modeling of CO2 based heat pumping systems*. PhD Thesis, Norwegian University of Science and Technology, Trondheim, Norway. 2009.
- [9] ASHRAE. *Chapter 37: Solar Energy Equipment*, in *ASHRAE Handbook - Heating, Ventilating, and Air-Conditioning Systems and Equipment (SI Edition)*. American Society of Heating, Refrigerating and Air-Conditioning Engineers, Inc. 2012.
- [10] S. Skogestad and C. Grimholt. *Chapter 5: The SIMC Method for Smooth PID Controller Tuning*, in *PID Control in the Third Millennium*. Springer London. 2012.
- [11] M. Otter, K.-E. Årzén, and I. Dressler. *StateGraph-A Modelica Library for Hierarchical State Machines*. 4th International Modelica Conference, Hamburg, Germany. March 7-8, 2005.
- [12] H. Li, Q. Sun, Q. Zhang, and F. Wallin. *A review of the pricing mechanisms for district heating systems*. Renewable and Sustainable Energy Reviews, 2015. 42: p. 56-65.